LETTER

Corrected: Author Correction

https://doi.org/10.1038/s41586-019-1546-z

Targeting cardiac fibrosis with engineered T cells

Haig Aghajanian[1,2,3], Toru Kimura[4], Joel G. Rurik[1,2,3], Aidan S. Hancock[1,2,3], Michael S. Leibowitz[5,6], Li Li[1,2,3], John Scholler[7], James Monslow[8], Albert Lo[8], Wei Han[9], Tao Wang[2], Kenneth Bedi[2,4], Michael P. Morley[2,4], Ricardo A. Linares Saldana[1,2,3], Nikhita A. Bolar[1,2,3], Kendra McDaid[2], Charles-Antoine Assenmacher[10], Cheryl L. Smith[1,2,3], Dagmar Wirth[11], Carl H. June[7], Kenneth B. Margulies[2,4], Rajan Jain[1,2,3,4], Ellen Puré[8], Steven M. Albelda[4] & Jonathan A. Epstein[1,2,3,4]*

Fibrosis is observed in nearly every form of myocardial disease[1]. Upon injury, cardiac fibroblasts in the heart begin to remodel the myocardium by depositing excess extracellular matrix, resulting in increased stiffness and reduced compliance of the tissue. Excessive cardiac fibrosis is an important factor in the progression of various forms of cardiac disease and heart failure[2]. However, clinical interventions and therapies that target fibrosis remain limited[3]. Here we demonstrate the efficacy of redirected T cell immunotherapy to specifically target pathological cardiac fibrosis in mice. We find that cardiac fibroblasts that express a xenogeneic antigen can be effectively targeted and ablated by adoptive transfer of antigen-specific CD8$^+$ T cells. Through expression analysis of the gene signatures of cardiac fibroblasts obtained from healthy and diseased human hearts, we identify an endogenous target of cardiac fibroblasts—fibroblast activation protein. Adoptive transfer of T cells that express a chimeric antigen receptor against fibroblast activation protein results in a significant reduction in cardiac fibrosis and restoration of function after injury in mice. These results provide proof-of-principle for the development of immunotherapeutic drugs for the treatment of cardiac disease.

Although quiescent fibroblasts are an important component of the normal structure of the myocardium, activated pathological fibroblasts induced by injury or disease negatively affect the compliance and stiffness of the tissue, and signal to cardiomyocytes to further negatively affect function[4]. Nevertheless, no therapies are known to directly target excessive fibrosis[5], despite the large burden of disease across the population. Furthermore, very few interventions have been shown to improve cardiac function and clinical outcomes in patients with impaired cardiac compliance and relaxation, which cause heart failure; including in patients who have heart failure with preserved ejection fraction[6]. However, genetic ablation of cardiac fibroblasts after hypertensive or ischaemic injury has previously been shown to reduce fibrosis and improve function in mice[7,8], providing further support for targeting fibroblasts directly.

Recently, breakthroughs in cancer therapy have been achieved by redirecting cytotoxic T cells to recognize specific antigens on cancer cells using either a modified T cell receptor[9] or a chimeric antigen receptor (CAR)[10]. The modified T cells are capable of effectively eliminating the cancer cells, and CAR T cell therapy has been approved by the FDA (US Food and Drug Administration)[11] for use in patients with some forms of leukaemia and lymphoma[12]. We and others[13,14] reasoned that engineered T cells could be used to target non-cancer cells, and we sought to determine whether activated cardiac fibroblasts could be effectively targeted by engineered T cells in a mouse model of heart disease.

In a first series of experiments, we generated mice in which a xenogeneic antigen (ovalbumin peptide (OVA))[15,16] that is not normally found in mice could be conditionally presented on the surface of activated cardiac fibroblasts. To induce expression of OVA, we used a tamoxifen-inducible Cre recombinase targeted to the periostin locus (*Postn*^{MCM}). *Postn* has previously been shown to be expressed by activated cardiac fibroblasts induced by injury, but is not expressed by quiescent cardiac fibroblasts[8]. To induce injury and fibrosis, *Rosa*^{OVA};*Postn*^{MCM} mice were continuously infused with angiotensin II and phenylephrine (AngII/PE) for 28 days through an osmotic mini-pump. Tamoxifen was administered at regular intervals by intraperitoneal injection to ensure near constant induction of Cre recombinase and expression of OVA (Fig. 1a). AngII/PE administration has been widely demonstrated to induce considerable cardiac fibrosis and dysfunction in mice by increasing afterload, chronotropy and direct effects on cardiomyocytes and cardiac fibroblasts[7,8]. Consistent with previous reports that demonstrate a peak of cardiac fibrosis within 1 week of this type of injury, we observed significant and widespread fibrosis throughout the myocardium of *Rosa*^{OVA};*Postn*^{MCM} mice 1 week after exposure to AngII/PE (Extended Data Fig. 1a). To selectively target OVA-expressing cardiac fibroblasts and their derivatives, we performed adoptive transfer of CD8$^+$ T cells that express a cognate T cell receptor against the OVA peptide (CD8$^+$ OT-I T cells)[17,18] in a cohort of mice at this time point (1 week after AngII/PE initiation) once pathological fibrosis was established. Control mice included *Rosa*^{OVA};*Postn*^{MCM} mice that received AngII/PE and tamoxifen, as well as OVA$^+$ mice that lack the *Postn*^{MCM} allele that received AngII/PE, tamoxifen and CD8$^+$ OT-I cells ($n \geq 6$ mice per cohort). At week 4, we observed continued widespread cardiac fibrosis in the control mice. By contrast, there was significantly less cardiac fibrosis in the tamoxifen-treated *Rosa*^{OVA};*Postn*^{MCM} mice that received OT-I T cells (Fig. 1b, c). In addition to the reduced fibrosis, a measure of cardiac hypertrophy—the heart weight to body weight ratio—was partially rescued after adoptive transfer of OT-I T cells in *Rosa*^{OVA};*Postn*^{MCM} mice (Extended Data Fig. 1b, c).

Having demonstrated that immunologically targeting and depleting activated cardiac fibroblasts is possible, we sought to identify endogenous proteins expressed by activated cardiac fibroblasts, but not by quiescent fibroblasts or other critical cell types, that could be specifically targeted as antigens by engineering (or genetically modifying) T cells. We analysed gene-expression data from an RNA-sequencing database consisting of 238 left ventricular tissue samples of human heart transplant donors and recipients. We found several fibroblast-specific genes[19,20] that were upregulated in the myocardium of patients with either hypertrophic cardiomyopathy (HCM) or dilated cardiomyopathy (DCM) compared to control, non-failing donor hearts (Fig. 2a and Extended Data Fig. 2a). Fibroblast activation protein (FAP) showed the greatest fold change in expression and upregulation when comparing either DCM or HCM samples to controls. FAP is a cell-surface glycoprotein[21] that has previously been shown to be expressed during

[1]Department of Cell and Developmental Biology, Perelman School of Medicine, University of Pennsylvania, Philadelphia, PA, USA. [2]Penn Cardiovascular Institute, Perelman School of Medicine, University of Pennsylvania, Philadelphia, PA, USA. [3]Institute for Regenerative Medicine, Perelman School of Medicine, University of Pennsylvania, Philadelphia, PA, USA. [4]Department of Medicine, Perelman School of Medicine, University of Pennsylvania, Philadelphia, PA, USA. [5]Department of Pediatrics, Perelman School of Medicine, University of Pennsylvania, Philadelphia, PA, USA. [6]Division of Oncology, The Children's Hospital of Philadelphia, Philadelphia, PA, USA. [7]Center for Cellular Immunotherapies, Perelman School of Medicine, University of Pennsylvania, Philadelphia, PA, USA. [8]Department of Biomedical Sciences, School of Veterinary Medicine, University of Pennsylvania, Philadelphia, PA, USA. [9]Echocardiography Laboratory, Hospital of the University of Pennsylvania, Philadelphia, PA, USA. [10]Department of Pathobiology, School of Veterinary Medicine, University of Pennsylvania, Philadelphia, PA, USA. [11]Model Systems for Infection and Immunity, Helmholtz Centre for Infection Research, Braunschweig, Germany. *e-mail: epsteinj@upenn.edu

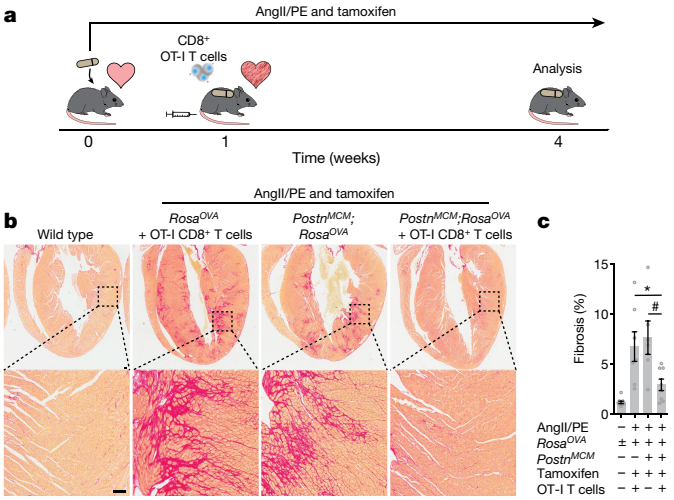

Fig. 1 | Redirected T cells can ablate cardiac fibroblasts. a, Schematic of cardiac injury and T cell-mediated cardiac fibroblast ablation. Mice were continuously administered AngII/PE through an osmotic minipump to induce cardiac injury and fibrosis, and injected with tamoxifen to trigger Cre-mediated OVA expression in the cardiac fibroblasts. $CD8^+$ OT-I T cells were adoptively transferred 1 week after pump implantation when fibrosis was already established, and mice were euthanized 4 weeks after implantation for analysis. **b**, Top, Picro-Sirius red staining of heart coronal sections to evaluate the level of fibrosis (red). Bottom, higher magnification image of left ventricular fibrosis. **c**, Quantification of ventricular fibrosis. Data are mean ± s.e.m. $*P = 0.0492$, $\#P = 0.0157$, one-way analysis of variance (ANOVA) between groups, $P = 0.0001$; Tukey's test was used for post hoc multiple comparisons; $n = 10, 7, 6, 8$ biologically independent mice, from left to right. Scale bar, 100 μm.

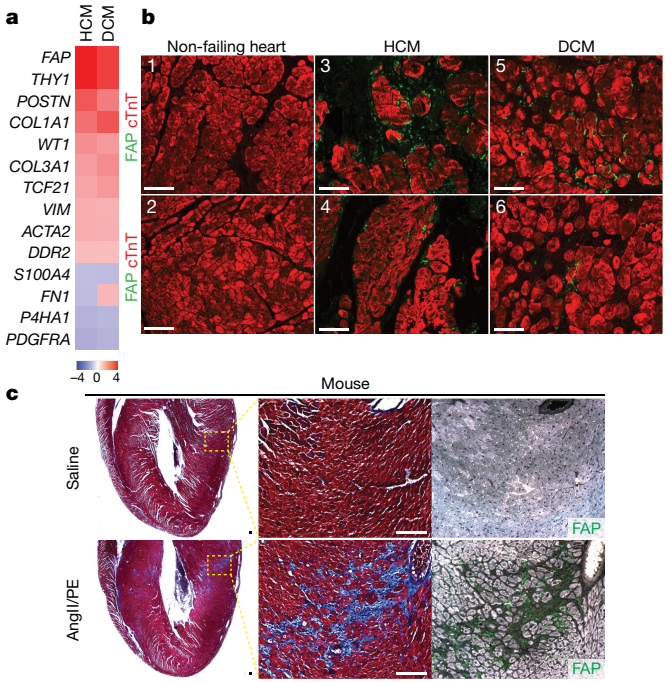

Fig. 2 | Human cardiac fibroblast targets in disease. a, Heat map of cardiac fibroblast gene-expression changes (fold change) in patients with HCM and DCM compared with non-failing hearts. $n = 122$ non-failing hearts, 27 HCM hearts, 89 DCM hearts. Differential gene expression was performed using a linear model. **b**, Immunohistochemistry of FAP (green) and cardiac troponin (cTnT) (cardiomyocytes, red) expression in left ventricular free-wall sections from six individual human samples of non-failing hearts (1 and 2), HCM (3 and 4) and DCM (5 and 6). Representative images of two independent experiments, showing similar results. **c**, Masson's trichrome stain of fibrosis (blue; left, centre) and immunohistochemistry of FAP (green; right) in adjacent wild-type mouse coronal heart sections 1 week after continuous saline (top) or AngII/PE (bottom) treatment. Representative images of two independent experiments, showing similar results. $n = 7$ biologically independent mice per group. Scale bars, 100 μm.

embryonic development at sites of active tissue remodelling such as during wound repair, in tissue fibrosis and in various tumours, but is expressed only at low levels—if at all—in most normal adult tissues in mice and humans[22,23]. FAP expression has been previously observed in human hearts following acute myocardial infarction injury[24]. We extended this finding by showing that FAP is robustly expressed by cardiac fibroblasts (and not by cardiomyocytes) in the left ventricular tissue of failing DCM and HCM human hearts (Fig. 2b and Extended Data Fig. 2b). Normal human hearts have minimal FAP expression (Fig. 2b). Thus, FAP is a potential candidate for targeting of pathological cardiac fibroblasts.

To test the feasibility of the use of FAP as an endogenous target of cardiac fibroblasts for immunotherapy, we returned to the AngII/PE model of hypertensive cardiac injury and fibrosis in mice. As we observed in our previous experiments, there is robust cardiac fibrosis as early as 1 week after AngII/PE infusion in C57BL/6 mice, and we confirmed that FAP is expressed by the activated cardiac fibroblasts in this model of injury (Fig. 2c and Extended Data Fig. 3a). Immunohistochemistry showed that FAP is not detectable in control hearts, with little to no expression elsewhere in the body, but is apparent in activated fibroblasts after 1 and 2 weeks of AngII/PE exposure as well as in tissue samples from additional models of cardiac injury, including myocardial infarction, transverse aortic constriction and muscular dystrophy (Fig. 2c and Extended Data Fig. 3b–d). To target and deplete FAP-expressing cardiac fibroblasts in the AngII/PE model, we adoptively transferred FAP CAR T cells at the 1- and 2-week time points after AngII/PE initiation (Fig. 3a). We administered a second injection of FAP CAR T cells in this set of experiments, owing to the short half-life of mouse FAP CAR T cells that has previously been observed in tumour models[25]. We detected FAP CAR T cells infiltrating the myocardium and co-localizing with FAP-expressing cardiac fibroblasts within 1 day of adoptive transfer (Extended Data Fig. 4a). By 4 weeks, there was a significant reduction in cardiac fibrosis in injured mice that had been treated with the FAP CAR T cells compared to controls (Fig. 3b, c) and fibrosis remained limited at 8 weeks in FAP CAR T cell-treated mice (1.92% ± 0.25, mean ± s.e.m., $n = 7$). Continued and widespread cardiac fibrosis was evident in each of the control mice that were exposed to AngII/PE, whereas fibrosis was reduced in all seven of the seven (and nearly eliminated in five of the seven) AngII/PE-exposed mice that were treated with FAP CAR T cells (Extended Data Fig. 4b–d). Along with the reduction in fibrosis, we observe a partial rescue of both systolic and diastolic cardiac function in injured mice treated with FAP CAR T cells compared to controls (Fig. 3d, e and Extended Data Fig. 5). Notably, we found persistence of perivascular fibrosis after treatment, consistent with the lack of FAP expression in perivascular fibroblasts (Extended Data Fig. 6a, b) that were induced by AngII/PE treatment.

CAR T cells against FAP have been used safely and effectively by multiple groups for cancer treatment studies in which mice are used[25–28] and have been administered to humans as part of a clinical trial for the treatment of mesothelioma[29]. Nevertheless, we performed extensive analysis of potential toxicities in our model system. We were not able to detect any histological effects of FAP CAR T cell therapy in numerous non-cardiac organs or tissues (Extended Data Fig. 6c), consistent with previous studies in which tumour stromal cells were targeted using FAP CAR T cells without apparent toxicities[25,27]. Serum cytokine levels, including expression of interleukin-2 and interleukin-6, were increased after AngII/PE administration; however, adoptive transfer of FAP CAR T cells did not further increase cytokine levels, which we monitored for 12 weeks after AngII/PE treatment (Extended Data Fig. 7). To determine whether treatment with FAP CAR T cells might be cardiotoxic, we used a commercially available cardiotoxicity array to interrogate 84 genes associated with myocardial toxicity. At 4 weeks after

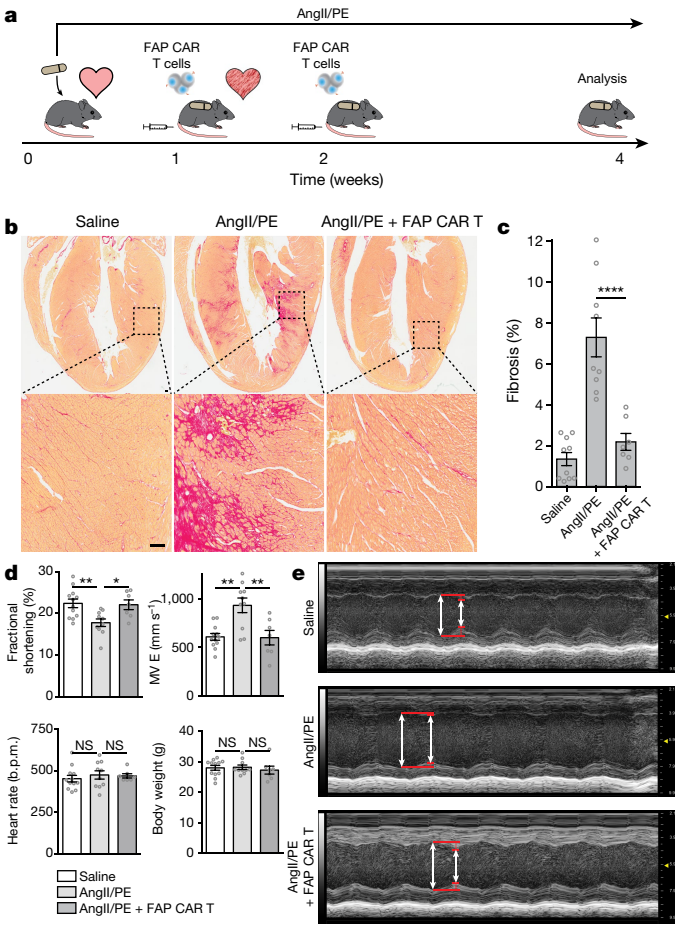

Fig. 3 | FAP CAR T cells can target cardiac fibrosis. a, Schematic of experiments for FAP CAR T cell targeting of cardiac fibroblasts. C57BL/6 mice were continuously administered AngII/PE through an osmotic minipump to induce cardiac injury and fibrosis. FAP CAR T cells were adoptively transferred 1 and 2 weeks after pump implantation when fibrosis had already been established. Mice were evaluated and euthanized at 4 weeks to assess fibrosis. **b**, Top, Picro-Sirius red staining of heart coronal sections in mice treated with saline (left), AngII/PE (centre) or AngII/PE and FAP CAR T cells (right) to evaluate fibrosis (red). Bottom, magnification of left ventricular fibrosis. Scale bar, 100 μm. **c**, Quantification of cardiac fibrosis. $^{****}P < 0.0001$; one-way ANOVA between groups, $P < 0.0001$; Tukey's test was used for post hoc multiple comparisons; $n = 10$, 9 and 7 biologically independent mice, from left to right. **d**, Comparison of cardiac functional parameters and body weight between experimental and control groups. $^{**}P < 0.01$, $^{*}P < 0.05$; NS, not significant; one-way ANOVA between groups; post hoc multiple comparisons on significant ($P < 0.05$) ANOVA, Tukey's test, $n = 10$, 9, 7 biologically independent mice, respectively). Specific P values can be found in the Source Data associated with this figure. MV E, mitral valve early (E) inflow velocity. **e**, M mode echocardiography of mice treated with saline (top), AngII/PE (middle) or AngII/PE and FAP CAR T cells (bottom). Arrows indicate systole and diastole and highlight the difference. Representative images of two independent experiments, showing similar results. Data are mean ± s.e.m.

AngII/PE treatment, differences in gene expression between AngII/PE and AngII/PE plus FAP CAR T cell-treated mice were noted, although these changes in expression were only partially consistent with cardiotoxicity (Extended Data Fig. 8a). These differences resolved by 8 weeks after AngII/PE treatment (Extended Data Fig. 8b). Furthermore, we assessed the expression levels of 1,659 inflammatory and immune genes and found that only 22 genes were differentially expressed between AngII/PE and AngII/PE plus FAP CAR T cell conditions at 4 weeks, which suggests that only very mild inflammation had occurred (Extended Data Fig. 8c). Immunohistological analysis of immune-cell infiltration revealed no significant differences in $CD3^+$, $CD4^+$, $CD8^+$ or MPO^+ cells, a reduction in $CD19^+$ cells, and an increase in $F4/80^+$ macrophages in AngII/PE and FAP CAR T compared with AngII/PE-treated samples at 4 weeks (Extended Data Fig. 8d). All FAP CAR T cell-treated mice survived to 12 weeks with no evidence of toxicity (Extended Data Fig. 9a–c).

In separate experiments, we examined the effect of FAP CAR T therapy on wound healing as FAP is expressed by some (but not all) fibroblasts in the skin[30]. No delays or defects in wound healing were observed in FAP CAR T cell-treated versus control-treated mice (Extended Data Fig. 9d–f), consistent with the presence of multiple fibroblast populations in various tissues—some of which do not express FAP[31]. Although rare FAP-expressing cells have been reported in the pancreas, no change in serum amylase levels were observed in response to FAP CAR T cell treatment (Extended Data Fig. 9g).

These results provide proof-of-concept for the possibility of targeting cardiac fibrosis in mice with engineered T cells[32] and immunotherapy. However, before this approach can be translated to humans, much work remains to determine whether FAP is the optimal target for treatment and that safety risks are minimized (Supplementary Table 1). Additionally, specific CAR constructs against the same antigen can have vastly different affinities, efficacies and safety profiles[25,27,33]. Continued investigation to identify unique antigens that are expressed by activated cardiac fibroblasts may identify alternative antigens, or combinations of antigens, that may be effective as targets for immunotherapy in patients with heart disease. As with any T cell therapy, off-target effects can range from mild to serious[34,35]. It may be necessary to engineer modified T cells with a 'kill switch' to limit the time of survival to minimize any off-target side effects. These approaches are under development[36]. Enormous progress in the treatment of certain cancers has been achieved through the use of engineered T cells. Here we suggest that the 'immunorevolution' may extend beyond oncology to affect one of the most common forms of human morbidity and mortality—heart disease.

Online content

Any methods, additional references, Nature Research reporting summaries, source data, extended data, supplementary information, acknowledgements, peer review information; details of author contributions and competing interests; and statements of data and code availability are available at https://doi.org/10.1038/s41586-019-1546-0

Received: 26 November 2018; Accepted: 8 August 2019;
Published online 11 September 2019.

1. Travers, J. G., Kamal, F. A., Robbins, J., Yutzey, K. E. & Blaxall, B. C. Cardiac fibrosis: the fibroblast awakens. *Circ. Res.* **118**, 1021–1040 (2016).
2. Kong, P., Christia, P. & Frangogiannis, N. G. The pathogenesis of cardiac fibrosis. *Cell. Mol. Life Sci.* **71**, 549–574 (2014).
3. Fang, L., Murphy, A. J. & Dart, A. M. A clinical perspective of anti-fibrotic therapies for cardiovascular disease. *Front. Pharmacol.* **8**, 186 (2017).
4. Ottaviano, F. G. & Yee, K. O. Communication signals between cardiac fibroblasts and cardiac myocytes. *J. Cardiovasc. Pharmacol.* **57**, 513–521 (2011).
5. Fan, Z. & Guan, J. Antifibrotic therapies to control cardiac fibrosis. *Biomater. Res.* **20**, 13 (2016).
6. Lam, C. S. P., Voors, A. A., de Boer, R. A., Solomon, S. D. & van Veldhuisen, D. J. Heart failure with preserved ejection fraction: from mechanisms to therapies. *Eur. Heart J.* **39**, 2780–2792 (2018).
7. Kaur, H. et al. Targeted ablation of periostin-expressing activated fibroblasts prevents adverse cardiac remodeling in mice. *Circ. Res.* **118**, 1906–1917 (2016).
8. Kanisicak, O. et al. Genetic lineage tracing defines myofibroblast origin and function in the injured heart. *Nat. Commun.* **7**, 12260 (2016).
9. Schmitt, T. M., Ragnarsson, G. B. & Greenberg, P. D. T cell receptor gene therapy for cancer. *Hum. Gene Ther.* **20**, 1240–1248 (2009).
10. June, C. H., O'Connor, R. S., Kawalekar, O. U., Ghassemi, S. & Milone, M. C. CAR T cell immunotherapy for human cancer. *Science* **359**, 1361–1365 (2018).
11. Mullard, A. FDA approves first CAR T therapy. *Nat. Rev. Drug Discov.* **16**, 669 (2017).
12. Ghobadi, A. Chimeric antigen receptor T cell therapy for non-Hodgkin lymphoma. *Curr. Res. Transl. Med.* **66**, 43–49 (2018).
13. June, C. H. & Sadelain, M. Chimeric antigen receptor therapy. *N. Engl. J. Med.* **379**, 64–73 (2018).

14. Lim, W. A. & June, C. H. The principles of engineering immune cells to treat cancer. *Cell* **168**, 724–740 (2017).
15. Sandhu, U. et al. Strict control of transgene expression in a mouse model for sensitive biological applications based on RMCE compatible ES cells. *Nucleic Acids Res.* **39**, e1 (2011).
16. Cebula, M. et al. An inducible transgenic mouse model for immune mediated hepatitis showing clearance of antigen expressing hepatocytes by $CD8^+$ T cells. *PLoS ONE* **8**, e68720 (2013).
17. Hogquist, K. A. et al. T cell receptor antagonist peptides induce positive selection. *Cell* **76**, 17–27 (1994).
18. Clarke, S. R. et al. Characterization of the ovalbumin-specific TCR transgenic line OT-I: MHC elements for positive and negative selection. *Immunol. Cell Biol.* **78**, 110–117 (2000).
19. Ivey, M. J. & Tallquist, M. D. Defining the cardiac fibroblast. *Circ. J.* **80**, 2269–2276 (2016).
20. Tallquist, M. D. & Molkentin, J. D. Redefining the identity of cardiac fibroblasts. *Nat. Rev. Cardiol.* **14**, 484–491 (2017).
21. Scanlan, M. J. et al. Molecular cloning of fibroblast activation protein α, a member of the serine protease family selectively expressed in stromal fibroblasts of epithelial cancers. *Proc. Natl Acad. Sci. USA* **91**, 5657–5661 (1994).
22. Rettig, W. J. et al. Cell-surface glycoproteins of human sarcomas: differential expression in normal and malignant tissues and cultured cells. *Proc. Natl Acad. Sci. USA* **85**, 3110–3114 (1988).
23. Niedermeyer, J. et al. Mouse fibroblast activation protein: molecular cloning, alternative splicing and expression in the reactive stroma of epithelial cancers. *Int. J. Cancer* **71**, 383–389 (1997).
24. Tillmanns, J. et al. Fibroblast activation protein α expression identifies activated fibroblasts after myocardial infarction. *J. Mol. Cell. Cardiol.* **87**, 194–203 (2015).
25. Wang, L. C. et al. Targeting fibroblast activation protein in tumor stroma with chimeric antigen receptor T cells can inhibit tumor growth and augment host immunity without severe toxicity. *Cancer Immunol. Res.* **2**, 154–166 (2014).
26. Kakarla, S. et al. Antitumor effects of chimeric receptor engineered human T cells directed to tumor stroma. *Mol. Ther.* **21**, 1611–1620 (2013).
27. Lo, A. et al. Tumor-promoting desmoplasia is disrupted by depleting FAP-expressing stromal cells. *Cancer Res.* **75**, 2800–2810 (2015).
28. Schuberth, P. C. et al. Treatment of malignant pleural mesothelioma by fibroblast activation protein-specific re-directed T cells. *J. Transl. Med.* **11**, 187 (2013).
29. Petrausch, U. et al. Re-directed T cells for the treatment of fibroblast activation protein (FAP)-positive malignant pleural mesothelioma (FAPME-1). *BMC Cancer* **12**, 615 (2012).
30. Govindaraju, P., Todd, L., Shetye, S., Monslow, J. & Puré, E. CD44-dependent inflammation, fibrogenesis, and collagenolysis regulates extracellular matrix remodeling and tensile strength during cutaneous wound healing. *Matrix Biol.* **75–76**, 314–330 (2019).
31. Croft, A. P. et al. Distinct fibroblast subsets drive inflammation and damage in arthritis. *Nature* **570**, 246–251 (2019).
32. Fischbach, M. A., Bluestone, J. A. & Lim, W. A. Cell-based therapeutics: the next pillar of medicine. *Sci. Transl. Med.* **5**, 179ps7 (2013).
33. Tran, E. et al. Immune targeting of fibroblast activation protein triggers recognition of multipotent bone marrow stromal cells and cachexia. *J. Exp. Med.* **210**, 1125–1135 (2013).
34. Cameron, B. J. et al. Identification of a titin-derived HLA-A1-presented peptide as a cross-reactive target for engineered MAGE A3-directed T cells. *Sci. Transl. Med.* **5**, 197ra103 (2013).
35. Linette, G. P. et al. Cardiovascular toxicity and titin cross-reactivity of affinity-enhanced T cells in myeloma and melanoma. *Blood* **122**, 863–871 (2013).
36. Sun, S., Hao, H., Yang, G., Zhang, Y. & Fu, Y. Immunotherapy with CAR-modified T Cells: toxicities and overcoming strategies. *J. Immunol. Res.* **2018**, 2386187 (2018).

METHODS

Mice. *Postn*^{MCM} mice were obtained from the laboratory of J. Molkentin[8]. *Rosa*^{OVA} mice show Cre-dependent expression of an intracellular OVA epitope that is presented by MHC I[15,16,37]. *Mdx/mTR*^{KO} mice were obtained from the laboratory of F. Mourkioti[38]. C57BL/6 mice were obtained from Charles River Laboratories. OT-I mice were obtained from The Jackson Laboratory. Sample sizes were determined by power calculations based on effect sizes previously reported in the literature. This study complied with all relevant ethical regulations and all mouse protocols were approved by the University of Pennsylvania Institutional Animal Care and Use Committee (IACUC).

Reagents and antibodies. Osmotic minipumps (Alzet, model 2004) were used for drug delivery. AngII (A9525-50MG), PE hydrochloride (P6126-10G), tamoxifen (T5648-1G) and corn oil (C8267) were obtained from Millipore Sigma. Picro-Sirius red stain kit (ab150681), anti-FAPα antibody (ab207178), anti-GFP antibody (ab6673) and anti-CD4 antibody (183685) were obtained from Abcam. Anti-vimentin antibody (9854), anti-F4/90 antibody (70076), anti-CD19 antibody (90176) and anti-CD8 antibody (98941) were obtained from Cell Signaling Technology. Anti-troponin T antibody (MS-295) was obtained from Thermo Fisher Scientific. Anti-CD3 antibody (MCA1477T) was obtained from Bio-Rad Laboratories. Anti-MPO antibody (A0398) was obtained from DAKO/Agilent. Sterile saline (0.9% sodium chloride, 00409488850) was obtained from Hospira.

Cardiac injury. All mice used in these experiments were adult males between 10 and 14 weeks of age. Wild-type mice were randomized to different conditions. AngII (1.5 μg/g/day) and PE (50 μg/g/day) or saline (0.9% sodium chloride) were continuously administered through osmotic minipumps (Alzet, 2004) for 28 days. Cre expression was induced in *Postn*^{MCM} mice by intraperitoneal injections of 100 μl of tamoxifen in corn oil (20 mg/ml). Injections were administered on alternating days for 1 week, and weekly afterward until euthanasia. Adoptive transfer of T cells was administered through tail vein or retro-orbital injection. Echocardiography was performed under isoflurane anaesthesia using a FUJIFILM VisualSonics system with an MS400 probe and Vevo 2100 software, and analyses were performed blinded to treatment group.

For myocardial infarction, mice were anaesthetized and a thoracotomy was performed by separating the fourth or fifth intercostal space to expose the heart. The pericardium was opened and an 8-0 nylon ligature, entering the heart on the left margin of the pulmonary cone and exiting near the insertion of the left auricular appendage was tied to the left anterior descending coronary artery to induce permanent myocardial infarction.

For transverse aortic constriction, mice were anaesthetized and antiseptic agents (betadine and 70% ethanol) were applied to the surgical area. The chest cavity was opened by an incision of the left second intercostal space. The transverse aorta was dissected from the surrounding tissues and a 7-0 silk suture was passed underneath the arch portion of the aorta and ligated for creation of stenosis of the aorta with about 50–70% lumen constriction.

Adoptive T cell transfer. Mouse T cells that express a CAR construct specific to mouse FAP (containing the scFv fragment from the specific mouse FAP antibody (clone 73.3)[25] coupled to the human CD3ζ and CD28 cytoplasmic domains) along with a small peptide that conferred resistance to adenosine- and prostaglandin E2-mediated suppression[39] or GFP were used. Infective particles were generated from the supernatants of Phoenix packaging cells (Allele; Phoenix Eco Cells Line ABP-RVC-10002; purchased from and authenticated by ATCC, CRL-3214; routinely tested negative for mycoplasma) transfected with retroviral vector plasmid and helper plasmids using Lipofectamine 2000 (Invitrogen), as previously described[25]. T cells were cultured in RPMI 1640 supplemented with 10% FBS, 100 U/ml penicillin, 100 μg/ml streptomycin sulfate, 1 mM pyruvate and 50 μM β-mercaptoethanol. Primary mouse T cells were isolated as suggested by the manufacturer (Miltenyi Biotec) from the spleens of mice and incubated in 12-well plates (2×10^6 cells per well in 2 ml T cell medium with 50 U/ml mouse interleukin (IL)-2 and Dynabeads Mouse T-Activator CD3/CD28 (Gibco, 11453D) in a 1:1 ratio). After 48 h, cells were plated in a 24-well plate coated with retrovirus and 5 μg/cm^2 of retronectin (Takara, T100B). Before plating T cells, a retronectin-coated 24-well plate was centrifuged without braking at room temperature for 1 h at 1,000*g* with 1 ml per well crude viral supernatant. After overnight incubation, cells were expanded with 50 U/ml IL-2 for 48 h. The transduction efficiency with muFAP CAR-RIAD (FAP CAR T cells), FAP–GFP-CAR or MigR1-GFP (control T cells) was assessed after transduction. We injected 10^7 CAR T cells per mouse.

For the OVA experiments, cells were obtained from C57BL/6 OT-I mouse spleens and purified using the mouse CD8a$^+$ T Cell Isolation Kit (Miltenyi Biotec, 130-104-075). Purity was assessed by flow cytometry. One week after injury, 5×10^6 CD8$^+$ T cells were adoptively transferred to mice.

Histology and immunohistochemistry. Mouse and human tissue samples were fixed overnight in 2–4% paraformaldehyde and dehydrated through an ethanol series. All samples were paraffin-embedded and sectioned. Haematoxylin and eosin (H&E) and Masson's trichrome staining was completed using a standard protocol. Picro-Sirius red staining was completed using a kit (Abcam, 150681) as per the manufacturer's instructions. In brief, sections were deparaffinized, incubated with Picro-Sirius red for 1 h, washed in acetic acid solution, washed in absolute alcohol, cleared with xylene and mounted. Slides were digitally scanned at 20× and analysed via colour deconvolution using ImageScope (Aperio) software. At least eight distinct sections were quantified to analyse the percentage fibrosis in the heart for each mouse in each condition.

Human cardiac expression data. Failing and non-failing human heart tissues were obtained from heart transplant recipients and from brain-dead organ donors. In situ cardioplegia was used for cardioprotection for all human heart procurements, as previously described[40,41]. In vivo echocardiography was performed before tissue collection for contemporaneous assessment of in vivo structure and function. Procurement of human myocardial tissue was performed with consent from all subjects and under protocols and ethical regulations approved by Institutional Review Boards at the University of Pennsylvania and the Gift-of-Life Donor Program (Pennsylvania, USA). Tissue specimens were frozen in liquid nitrogen and stored at –80 °C until used.

Total RNA was extracted from human cardiac tissue samples using the miRNeasy Kit (Qiagen) including DNase treatment. For RNA-sequencing analyses, library preparation was conducted using the Illumina truSeq stranded mRNA kit followed by the Nugen Ovation amplification kit. Resultant FASTQ files were assessed for quality control using the FastQC program. FASTQ files were aligned to the human reference genome (hGRC37/Hg19) using the STAR aligner[42]. Duplicate reads were flagged using the MarkDuplicates program of Picard tools. Per gene read counts for Ensembl (v.75) gene annotations were computed using the R package with duplicate reads removed. Gene counts represented as counts per million (CPM) were first nominalized using the TMM method in the edgeR R package and genes with 25% of samples with a CPM < 1 were removed and deemed to have low expression. The data were transformed using the VOOM function of the limma R package[43]. Differential gene expression was performed using a linear model using the limma package.

Cardiotoxicity assay. Total RNA was isolated from formalin-fixed, paraffin-embedded cardiac sections with the RNeasy FFPE kit (Qiagen, 73504, 19093). Samples were blinded to condition. cDNA was then prepared with the RT^2 PreAMP cDNA synthesis kit (Qiagen, 330451) and pre-amplified with assay-specific RT^2 PreAMP primer mix (Qiagen, 330241, PBM-095Z) according to the manufacturer's recommendations. Pre-amplified cDNA was then assayed using the mouse cardiotoxicity RT^2 profiler PCR array (Qiagen, 330231, PAMM095Z) with RT^2 SYBR Green ROX qPCR mastermix (Qiagen, 330523) on a real-time PCR StepOnePlus system (Applied Biosystems). The threshold was set consistently across the entire experiment. Measured C_t values were normalized to *Gapdh*, compared using a Welch's *t*-test and graphs were produced in R using the tidyverse suite of packages.

Cytokine assay. Blood was collected by cardiac puncture or via inferior vena cava during dissection at 10 days, 2 weeks (14 days), 4 weeks (28 days) and 12 weeks (84–88 days), allowed to clot and spun down to isolate serum. Blinded serum samples were assayed by multiplex technology (MAGPIX, Luminex) by overnight incubation using a mouse cytokine 25plex (mcytomag-70k-PMX, EMD Millipore).

Immune and inflammation assay. Immune and inflammation-related gene-expression analyses were done with the Immuno-Oncology assay (HTG Molecular Diagnostics). In brief, samples were obtained from formalin-fixed paraffin-embedded sections of hearts from mice that had been treated with AngII/PE and FAP CAR T cells or AngII/PE for 4 weeks ($n = 3$ per condition, samples were blinded before processing). The estimated mean value of each probe for each group was normalized using DESeq2 median normalization[44]. The *P* value for each probe was adjusted using the Benjamini and Hochberg method for controlling the false discovery rate[45]. The estimated mean value of each probe for each group after normalization is displayed as a volcano plot of the $\log_{10}$-transformed adjusted *P* value against the log-transformed fold change for each probe in the assay.

Wound-healing assay. In brief, 8–9-week-old C57BL/6 mice were anaesthetized using isoflurane and two equidistant 4-mm full-thickness excisional wounds were generated using circular biopsy punches in the dorsal skin approximately 5 mm below the shoulder blades. Mice were randomly assigned into two groups ($n = 6$ mice per group) and received 1×10^7 control or FAP-CAR-transduced mouse T cells intravenously immediately after wounding and 3 days after wounding. Body weight measurements were taken every other day along with imaging of the wounds using the IVIS Lumina III Bioluminescence and Fluorescence Imaging System (PerkinElmer). Mice were euthanized 8 days after wounding. Serum was collected to measure amylase levels as a read-out of pancreatic function. Skin samples were fixed in prefer fixative (Anatech), processed and stained with H&E. Digital images were captured on a Nikon TiE inverted microscope (Nikon Instruments). Wound closure was quantified using ImageJ software.

Statistics. Differences between two groups were compared using Student's or Welch's *t*-test. Differences between multiple groups were compared with one-way

ANOVA. Significant ANOVA results were further analysed by Tukey's multiple comparisons test.

Reporting summary. Further information on research design is available in the Nature Research Reporting Summary linked to this paper.

Data availability

All data are available from the corresponding author upon request.

37. Ochel, A. et al. Effective intrahepatic $CD8^+$ T-cell immune responses are induced by low but not high numbers of antigen-expressing hepatocytes. *Cell. Mol. Immunol.* **13**, 805–815 (2016).
38. Mourkioti, F. et al. Role of telomere dysfunction in cardiac failure in Duchenne muscular dystrophy. *Nat. Cell Biol.* **15**, 895–904 (2013).
39. Newick, K. et al. Augmentation of CAR T-cell trafficking and antitumor efficacy by blocking protein kinase A localization. *Cancer Immunol. Res.* **4**, 541–551 (2016).
40. Dipla, K., Mattiello, J. A., Jeevanandam, V., Houser, S. R. & Margulies, K. B. Myocyte recovery after mechanical circulatory support in humans with end-stage heart failure. *Circulation* **97**, 2316–2322 (1998).
41. Chen, C. Y. et al. Suppression of detyrosinated microtubules improves cardiomyocyte function in human heart failure. *Nat. Med.* **24**, 1225–1233 (2018).
42. Dobin, A. et al. STAR: ultrafast universal RNA-seq aligner. *Bioinformatics* **29**, 15–21 (2013).
43. Law, C. W., Chen, Y., Shi, W. & Smyth, G. K. voom: precision weights unlock linear model analysis tools for RNA-seq read counts. *Genome Biol.* **15**, R29 (2014).
44. Love, M. I., Huber, W. & Anders, S. Moderated estimation of fold change and dispersion for RNA-seq data with DESeq2. *Genome Biol.* **15**, 550 (2014).
45. Benjamini, Y. & Hochberg, Y. Controlling the false discovery rate: a practical and powerful approach to multiple testing. *J. R. Stat. Soc. B* **57**, 289–300 (1995).

Acknowledgements We thank J. Molkentin for sharing the *Postn*^{MCM} mice with us, A. Stout for help with imaging, D. Martinez for help with image analysis, M. Scherrer-Crosbie for guidance on the echocardiogram procedure and interpretation, F. Mourkioti for sharing the *mdx/mTR*^{KO} mice with us, E. Radaelli for help with immunohistochemistry and the University of Pennsylvania Diabetes Research Center (DRC) for the use of the RIA Biomarker Core (P30-DK19525). This research was supported by NIH R35 HL140018, T32 HL007843-22, F31 HL147416, the Burroughs Wellcome Fund to R.J., the Cotswold Foundation and the W. W. Smith Endowed Chair to J.A.E.

Author contributions H.A. and J.A.E. conceived the project and designed experiments. H.A., T.K., J.G.R., A.S.H., M.S.L., L.L., J.M., A.L., W.H., T.W., K.B., R.A.L.S., N.A.B., K.M., C.-A.A. and C.L.S. performed experiments and interpreted data. M.P.M. performed bioinformatic analysis and interpretation. J.S., R.J., D.W., C.H.J., K.B.M., E.P. and S.M.A. contributed reagents, analysis and interpretation. H.A. and J.A.E. wrote the manuscript. J.A.E. supervised all aspects of the research.

Competing interests C.H.J., E.P. and S.M.A. are inventors (University of Pennsylvania, Wistar Institute) on a patent for a FAP CAR (US Utility Patent 9,365,641 issued 14 June 2016, WIPO Patent Application PCT/US2013/062717). H.A. and J.A.E. are inventors (University of Pennsylvania) on a patent for the use of CAR T therapy in heart disease (US Provisional Patent Application 62/563,323 filed 26 September 2017, WIPO Patent Application PCT/US2018/052605). C.H.J. is a scientific founder and has equity in Tmunity Therapeutics, a biotech dedicated to developing engineered T cells for therapy of cancer, infections and autoimmunity, reports grants from Novartis and Tmunity Therapeutics and is on the scientific advisory boards of Immune Design, Viracta Therapeutics, Carisma Therapeutics and Cabaletta Bio.

Additional information

Supplementary information is available for this paper at https://doi.org/10.1038/s41586-019-1546-z.

Correspondence and requests for materials should be addressed to J.A.E.

Peer review information *Nature* thanks Jeffery D. Molkentin, Richard T. Lee and the other, anonymous, reviewer(s) for their contribution to the peer review of this work.

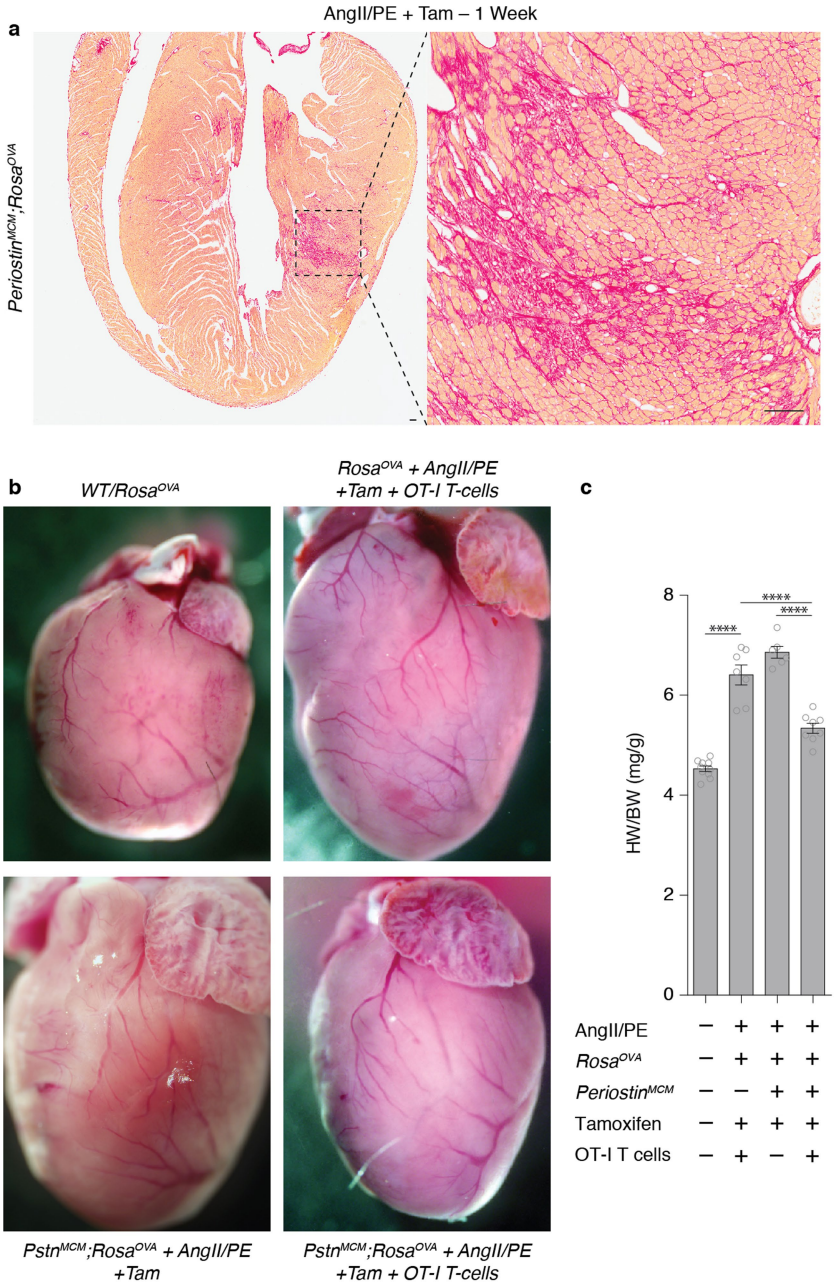

Extended Data Fig. 1 | Cardiac fibrosis and hypertrophy. a, Picro-Sirius red staining for cardiac fibrosis (red) in a coronal section of the heart of a *Postn*^{MCM};*Rosa*^{OVA} mouse treated with AngII/PE and tamoxifen for 1 week (left). High-powered field of the left ventricular free wall (right). Representative image of three biologically independent mice, showing similar results. Scale bars, 100 μm. **b**, Control and experimental hearts were measured (weight (mg)) and images captured. Representative images are shown. **c**, Quantification of heart weight to body weight (HW/BW) ratio of indicated genotypes and conditions. Data are mean ± s.e.m. ****$P < 0.0001$ (one-way ANOVA between groups, $P < 0.0001$; post hoc test for multiple comparisons, Tukey's test; $n = 10, 7, 6, 8$ biologically independent mice from left to right).

a

	HCM		DCM	
Gene Symbol	Fold Change	*P* Value	Fold Change	*P* Value
FAP	3.92	6.97E-28	3.11	3.12E-36
THY1	3.92	6.40E-20	3.12	5.07E-27
POSTN	2.64	1.40E-11	2.02	3.73E-13
COL1A1	2.22	1.83E-15	2.71	1.04E-41
WT1	1.74	6.29E-12	1.57	4.17E-16
COL3A1	1.53	1.28E-05	1.77	8.72E-18
TCF21	1.39	1.01E-05	1.59	5.26E-19
VIM	1.26	1.43E-12	1.20	1.60E-16
ACTA2	1.26	2.64E-03	1.22	7.16E-05
DDR2	1.05	0.21	1.02	0.47
S100A4	-1.00	0.96	-1.03	0.33
FN1	-1.01	0.90	1.11	0.06
P4HA1	-1.18	4.11E-04	-1.11	1.10E-03
PDGFRA	-1.25	1.40E-05	-1.17	9.98E-06

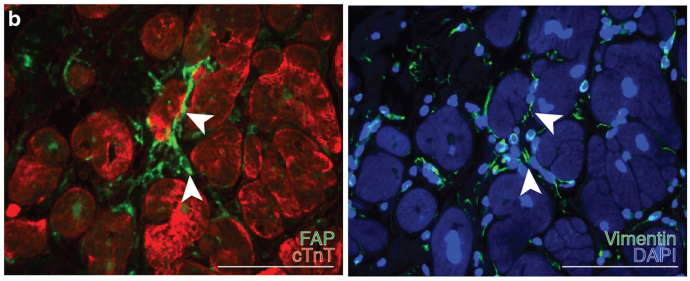

Extended Data Fig. 2 | Markers of activated cardiac fibroblasts in human disease. a, Fold change and *P* values of cardiac-fibroblast-specific gene expression of heart samples from patients with HCM and DCM compared with samples from non-failing hearts. $n = 122$ (non-failing), 27 (HCM) and 89 (DCM). Differential gene-expression analyses were performed using a linear model. **b**, Immunohistochemistry co-staining of cardiac troponin (red) and FAP (green; left) and vimentin (green; right) in adjacent sections from the left ventricle of a patient with DCM. FAP and vimentin are expressed in the same fibroblasts (arrowheads). Representative images of two independent experiments, showing similar results. Scale bars, 100 μm.

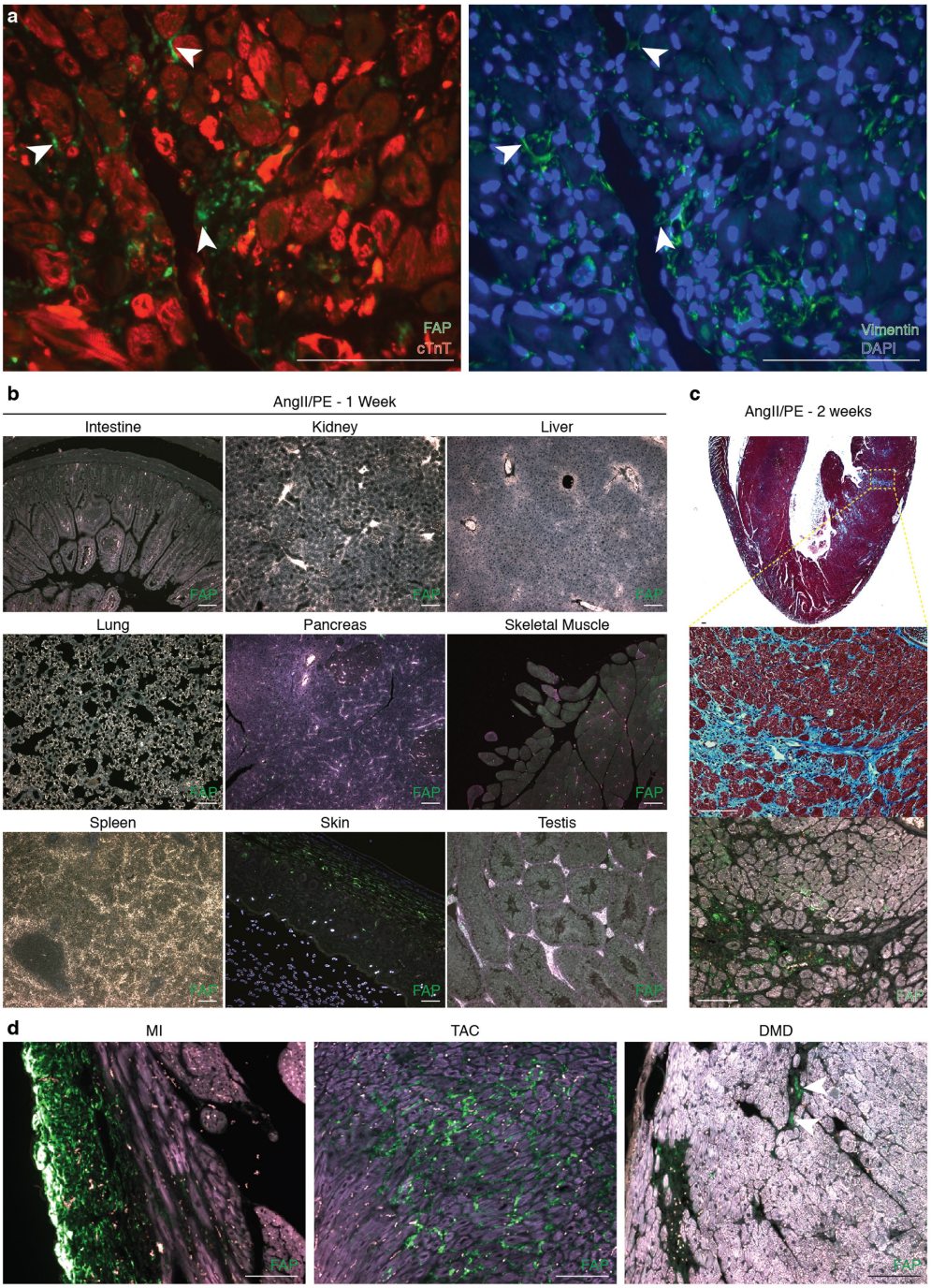

Extended Data Fig. 3 | FAP is expression in mouse cardiac fibroblasts after injury. a, Immunohistochemistry co-staining of cardiac troponin (red) and FAP (green; left) and vimentin (green; right) in adjacent sections from the left ventricle of a mouse treated with AngII/PE for 2 weeks. FAP and vimentin are expressed in the same fibroblasts (arrowheads). Representative images from two independent experiments, showing similar results ($n = 7$ biologically independent mice). **b**, Immunohistochemistry of FAP (green) in various organs or tissues after 1 week of AngII/PE treatment. Representative image of $n = 3$ biologically independent mice, showing similar results. **c**, Masson's trichrome stain for fibrosis (blue; top, centre) and immunohistochemistry of FAP (green; bottom) in coronal heart sections of a wild-type mouse 2 weeks after continuous AngII/PE treatment. Staining and immunohistochemistry were performed on adjacent sections. Bottom insets, higher magnification of left ventricular free wall. Representative image of two independent experiments, showing similar results ($n = 7$ biologically independent mice). **d**, Immunohistochemistry of FAP (green) in mouse models of cardiac injury. DMD, Duchenne's muscular dystrophy (*mdx/mTR*^{KO} G2 mice); MI, myocardial infarction; TAC, transverse aortic constriction. Scale bars, 100 μm.

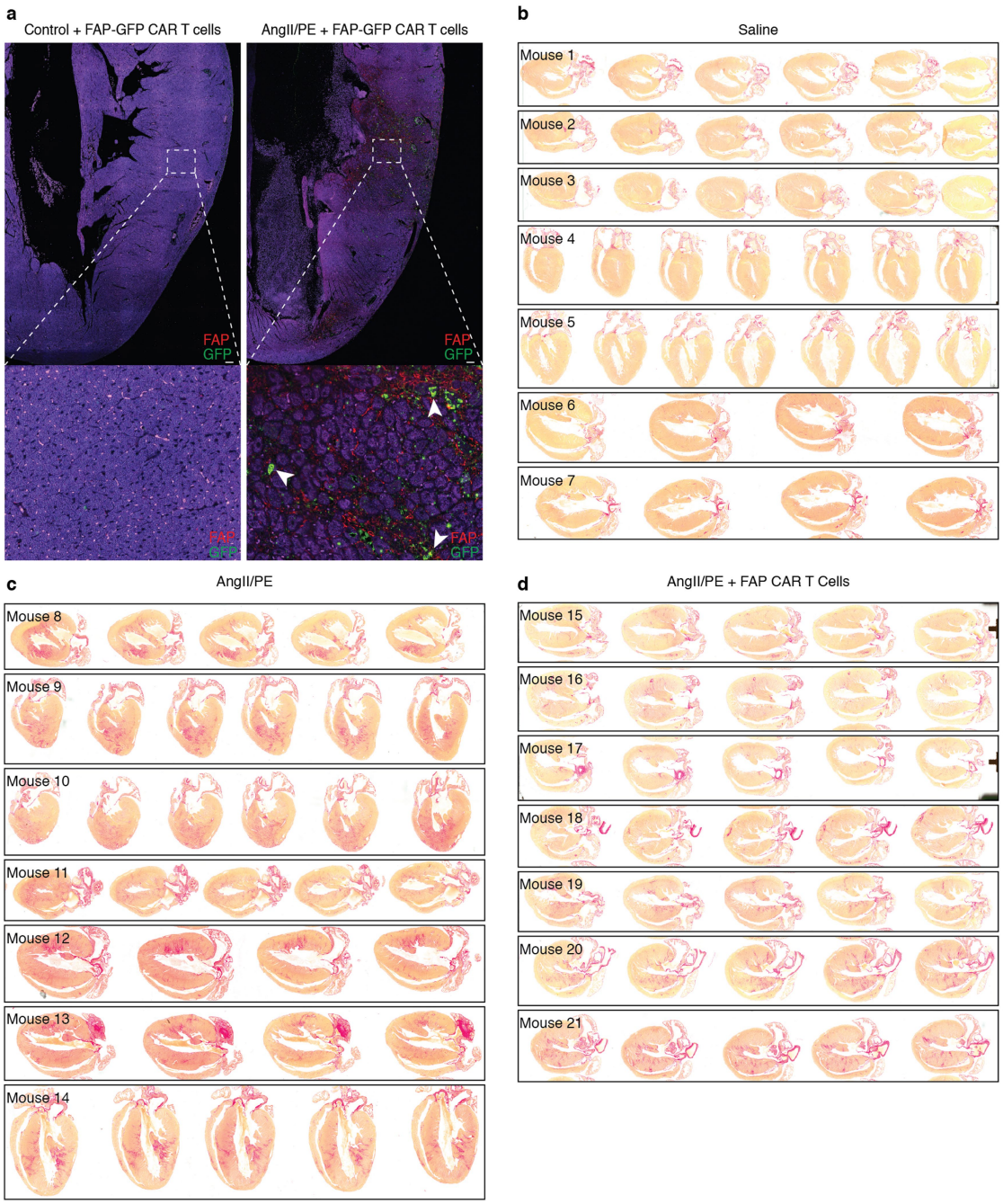

Extended Data Fig. 4 | FAP CAR T cells infiltrate the heart and reduce cardiac fibrosis. a, Immunohistochemistry of FAP (red) and GFP (green) on the left ventricular free wall of mouse heart coronal sections. Wild-type C57BL/6 mice were treated with (right) or without (left) AngII/PE for 1 week, injected with FAP–GFP CAR T cells and euthanized 1 day later. FAP–GFP CAR T cells co-localize with FAP-expressing cells (arrowheads, bottom). **b**–**d**, Picro-Sirius red staining of hearts from 21 individual mice (1–21) treated for 4 weeks with saline (**b**), AngII/PE (**c**) or AngII/PE and FAP CAR T cells (**d**) to assess fibrosis (red). Representative images of two independent experiments, showing similar results. Scale bars, 100 μm.

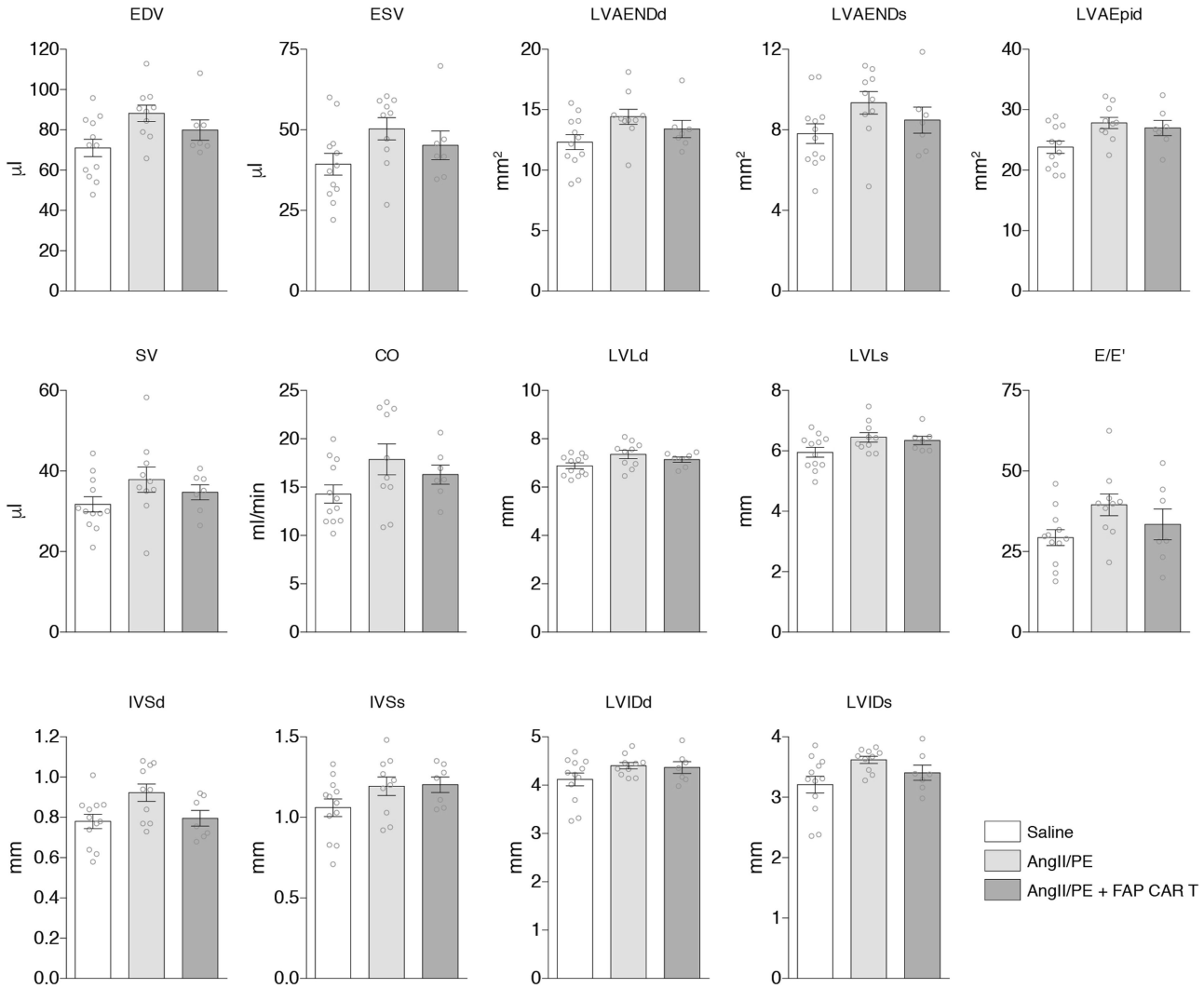

Extended Data Fig. 5 | Echocardiography after injury and treatment. Results from echocardiogram analyses of C57BL/6 mice treated for 4 weeks with saline, AngII/PE or AngII/PE and FAP CAR T cells ($n = 12$, 10 and 7 biologically independent mice, respectively). Data are mean ± s.e.m. CO, cardiac output; E/E′, ratio of mitral peak velocity of early filling (E) to early diastolic mitral annular velocity (E′); EDV, end diastolic volume; ESV, end systolic volume; FS, fractional shortening; HR, heart rate; IVSd, interventricular septal end diastole; IVSs, interventricular septal end systole; LVIDd, left ventricular internal diameter end diastole; LVIDs, left ventricular internal diameter end systole; LVLd, left ventricular endocardial length (diastole); LVLs, left ventricular endocardial length (systole); LVAEpid, left ventricular epicardial area (diastole); LVAENDd, left ventricular endocardial area (diastole); LVAENDs, left ventricular endocardial area (systole); MV E, early ventricular filling velocity; SV, stroke volume.

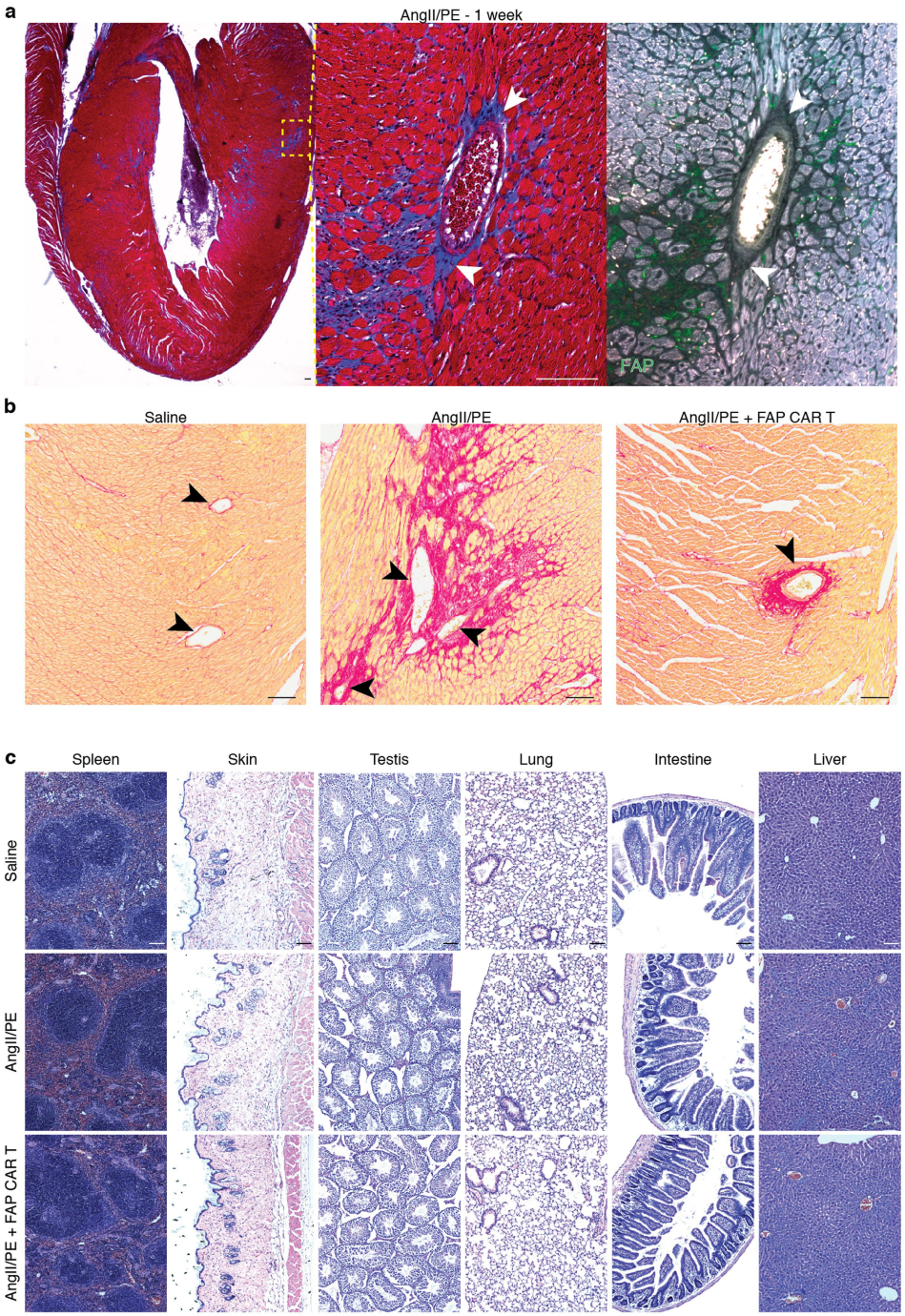

Extended Data Fig. 6 | FAP CAR T treatment does not affect perivascular fibrosis or other organs. a, Masson's trichrome stain (blue; left, centre) and FAP immunohistochemistry (green; right) on adjacent heart coronal sections 1 week after commencement of continuous AngII/PE treatment. FAP expression is present in interstitial, but not perivascular, fibroblasts (white arrowheads). Image is centred on the vessel shown in Fig. 2c. Representative images of two independent experiments, showing similar results. **b**, Picro-Sirius red staining of perivascular fibrosis (black arrowheads, red) in heart coronal sections from mice treated for 4 weeks with saline, AngII/PE or AngII/PE and FAP CAR T cells. Representative images of two independent experiments with similar results. **c**, H&E staining of various tissue sections from mice treated for 4 weeks with saline, AngII/PE or AngII/PE and FAP CAR T cells. Representative images of two independent experiments, showing similar results. Scale bars, 100 μm.

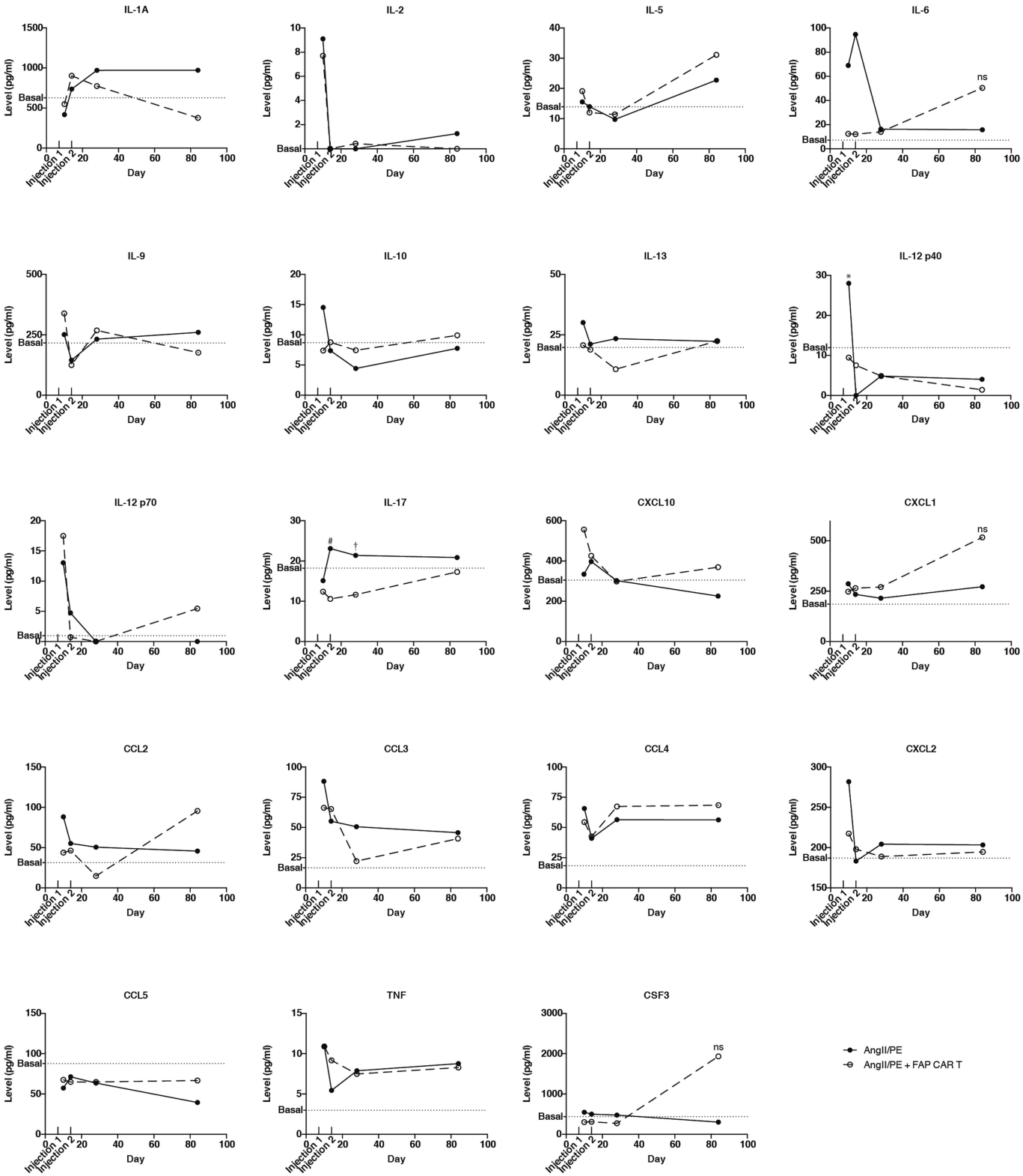

Extended Data Fig. 7 | Long-term serum cytokine levels after FAP CAR T cell treatment. Serum cytokine levels in mice treated with either AngII/PE or AngII/PE and FAP CAR T cells over 12 weeks. FAP CAR T cells were injected at 1 and 2 weeks as indicated. Levels were assessed at 10 days, 2 weeks, 4 weeks and 12 weeks. Basal levels were determined by the average cytokine levels of three untreated mice. INFγ and IL-4 were below the limit of detection in all conditions. $^{*}P = 0.019$, $^{\#}P = 0.035$, $^{\dagger}P = 0.045$; two-tailed unpaired Student's *t*-test; $n = 3$ biologically independent mice per condition.

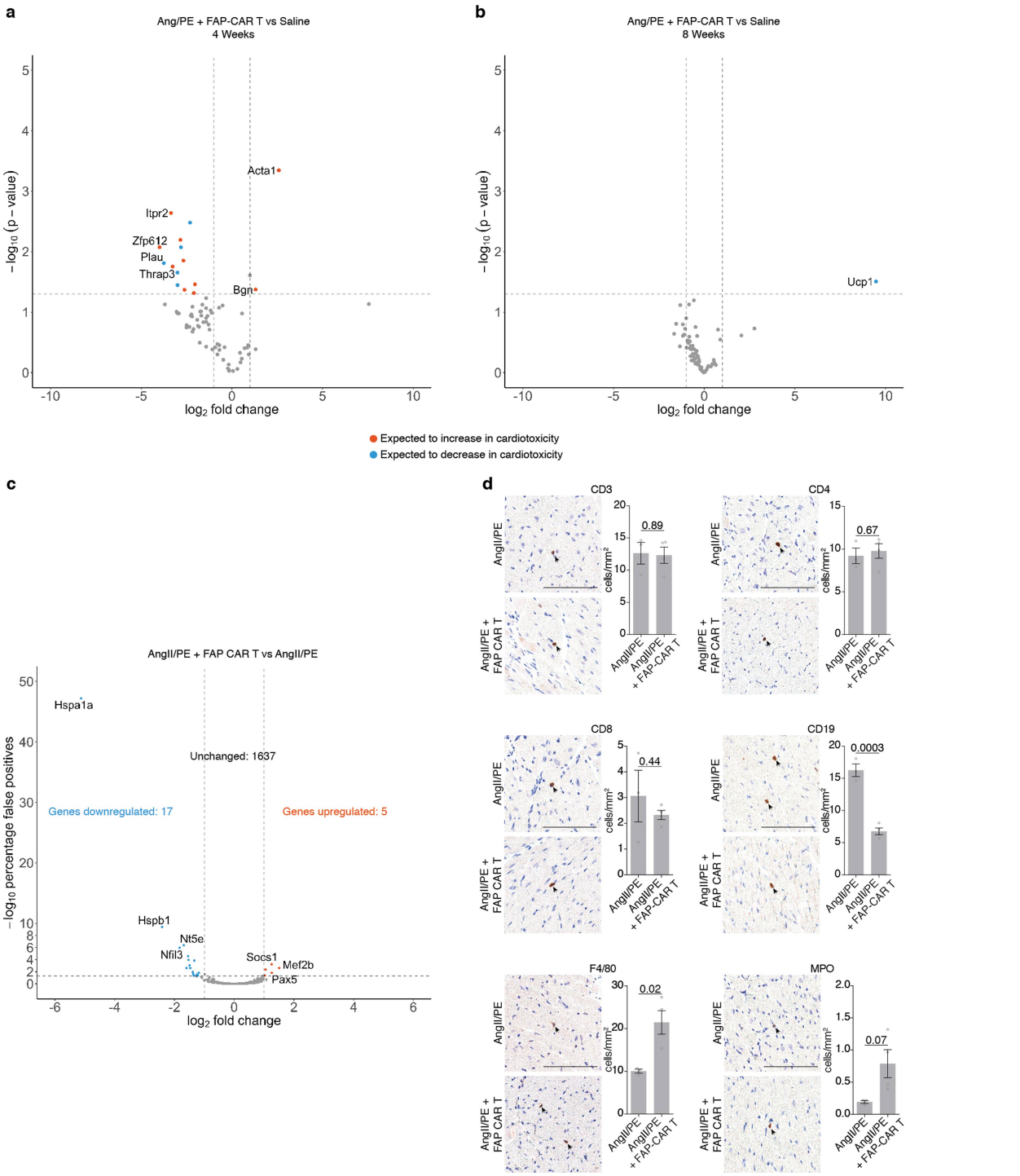

Extended Data Fig. 8 | Cardiotoxicity, inflammation and immune assessments after FAP CAR T cell transfer. a, Volcano plot showing the differential expression of genes known to be modified in cardiotoxicity in the hearts of mice treated with either AngII/PE and FAP CAR T cells or a saline control for 4 weeks. Statistically significant changes are marked to indicate whether genes are expected to increase (orange) or decrease (blue) in the setting of cardiotoxicity. **b**, Differential expression of the same conditions in **a** at 8 weeks. **a**, **b**, Two-sided Welch's *t*-test; $n = 3$ biologically independent mice per condition. **c**, Volcano plot showing the differential expression of 1,659 immune- and inflammation-related genes from hearts of mice treated with AngII/PE and FAP CAR T cells or AngII/PE for 4 weeks. In total, 22 genes were differentially expressed between the conditions. $n = 3$ mice per condition. **d**, Photomicrographs and quantification (mean ± s.e.m.) of immune cell (arrowheads) residency of the left ventricle at 4 weeks after either AngII/PE or AngII/PE and FAP CAR T cell treatment. Two-tailed unpaired Student's *t*-test; $n = 3$ or 4 biologically independent mice, respectively. Scale bars, 100 μm.

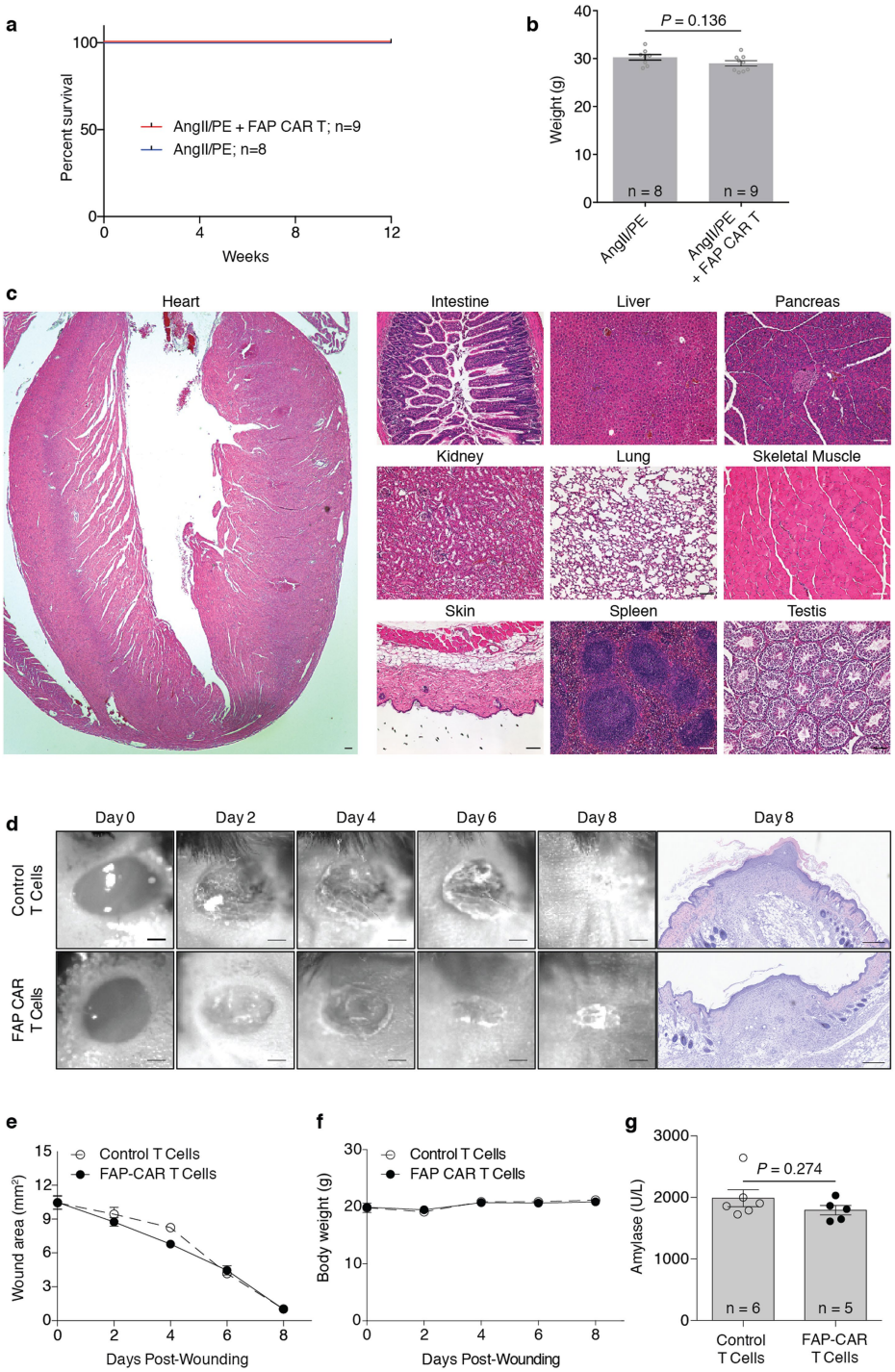

Extended Data Fig. 9 | Assessment of safety and toxicity following FAP CAR T cell transfer. a, Kaplan–Meier survival curve of mice treated with either AngII/PE or AngII/PE and FAP CAR T cells for 12 weeks. **b**, Body weight measurements at 12 weeks. Two-tailed unpaired Student's *t*-test. **c**, H&E of sections of heart and organs or tissues at 12 weeks from a mouse treated with AngII/PE and FAP CAR T cells. Representative images of $n = 3$ independent mice, showing similar results. Scale bars, 100 μm. **d**, Photomicrographs and H&E sections of a healing wound over 8 days in mice treated with either FAP CAR or control T cells immediately and 3 days after wounding. Scale bars, 1 mm (wounds) and 250 μm (H&E sections). **e**, **f**, Quantification of wound area (**e**) and measurements of body weight (**f**). **g**, Serum levels of amylase at day 8 to test pancreatic toxicity. Data are mean ± s.e.m.

nature research

Corresponding author(s): Jonathan A. Epstein

Reporting Summary

Nature Research wishes to improve the reproducibility of the work that we publish. This form provides structure for consistency and transparency in reporting. For further information on Nature Research policies, see Authors & Referees and the Editorial Policy Checklist.

Statistical parameters

When statistical analyses are reported, confirm that the following items are present in the relevant location (e.g. figure legend, table legend, main text, or Methods section).

n/a	Confirmed	
☐	☒	The exact sample size (*n*) for each experimental group/condition, given as a discrete number and unit of measurement
☐	☒	An indication of whether measurements were taken from distinct samples or whether the same sample was measured repeatedly
☐	☒	The statistical test(s) used AND whether they are one- or two-sided *Only common tests should be described solely by name; describe more complex techniques in the Methods section.*
☒	☐	A description of all covariates tested
☐	☒	A description of any assumptions or corrections, such as tests of normality and adjustment for multiple comparisons
☐	☒	A full description of the statistics including central tendency (e.g. means) or other basic estimates (e.g. regression coefficient) AND variation (e.g. standard deviation) or associated estimates of uncertainty (e.g. confidence intervals)
☒	☐	For null hypothesis testing, the test statistic (e.g. *F*, *t*, *r*) with confidence intervals, effect sizes, degrees of freedom and *P* value noted *Give P values as exact values whenever suitable.*
☒	☐	For Bayesian analysis, information on the choice of priors and Markov chain Monte Carlo settings
☒	☐	For hierarchical and complex designs, identification of the appropriate level for tests and full reporting of outcomes
☒	☐	Estimates of effect sizes (e.g. Cohen's *d*, Pearson's *r*), indicating how they were calculated
☐	☒	Clearly defined error bars *State explicitly what error bars represent (e.g. SD, SE, CI)*

Our web collection on statistics for biologists may be useful.

Software and code

Policy information about availability of computer code

Data collection	Nikon NIS-Elements D 3.00, Olympus DP controller 3.1.1.267, Fujifilm VisualSonics VEVO 2100, PerkinElmer IVIS Lumina III Bioluminescence and Fluorescence Imaging System 4.2.0.14335, Luminex Exponent 4.2, and Leica LAS X 3.5.2.18963
Data analysis	Leica Aperio Imagescope 12.4, Graphpad Prism 6, Imagej 2.0.0, R 3.5, FastQC 0.11.7, STAR aligner 2.5.4b, Picard Tools 2.17.11, BioConductor 3.8, edgeR 3.24.3, limma 3.38.3, Ensemble v75, Human reference genome hGRC37/Hg19, Tidyverse 1.2.1, DEseq2 1.14.1

For manuscripts utilizing custom algorithms or software that are central to the research but not yet described in published literature, software must be made available to editors/reviewers upon request. We strongly encourage code deposition in a community repository (e.g. GitHub). See the Nature Research guidelines for submitting code & software for further information.

Data

Policy information about availability of data

All manuscripts must include a data availability statement. This statement should provide the following information, where applicable:

- Accession codes, unique identifiers, or web links for publicly available datasets
- A list of figures that have associated raw data
- A description of any restrictions on data availability

The datasets generated during and/or analyzed during the current study are available from the corresponding author on reasonable request.

Field-specific reporting

Please select the best fit for your research. If you are not sure, read the appropriate sections before making your selection.

☒ Life sciences ☐ Behavioural & social sciences ☐ Ecological, evolutionary & environmental sciences

For a reference copy of the document with all sections, see nature.com/authors/policies/ReportingSummary-flat.pdf

Life sciences study design

All studies must disclose on these points even when the disclosure is negative.

Sample size	Sample sizes were determined by power calculations based on effect sizes previously reported in the literature.
Data exclusions	Any mice that experienced complications from surgery were excluded from proceeding with the experiments. This was predetermined criteria before commencing experiments to limit confounding variables.
Replication	Experiments were replicated in multiple instances. All attempts at replication were successful.
Randomization	WT mice were randomized to different conditions. All mice were age, sex, and strain matched.
Blinding	Echocardiograms were blinded. Inflammation arrays were blinded to the company performing them. Cardiotoxicity assay was blinded prior to sample processing. Radioimmune assays for cytokines were blinded. All analysis was performed in a uniform and unbiased fashion.

Reporting for specific materials, systems and methods

Materials & experimental systems

n/a	Involved in the study
☐	☒ Unique biological materials
☐	☒ Antibodies
☐	☒ Eukaryotic cell lines
☒	☐ Palaeontology
☐	☒ Animals and other organisms
☐	☒ Human research participants

Methods

n/a	Involved in the study
☒	☐ ChIP-seq
☒	☐ Flow cytometry
☒	☐ MRI-based neuroimaging

Unique biological materials

Policy information about availability of materials

Obtaining unique materials	There are no restrictions.

Antibodies

Antibodies used	Rabbit anti-fibroblast activation protein, alpha (Abcam, ab207178) Clone-EPR20021 (1:100) Goat anti-GFP (Abcam, ab6673) Polyclonal (1:100) Rabbit anti-CD4 (Abcam, 183685) Clone-EPR19514 (1:500) Rabbit anti-Vimentin-AlexaFluor 488 Conjug. (Cell Signaling Technology, 9854) Clone-D21H3 (1:100) Rabbit anti-F4/80 (Cell Signaling Technology, 70076) Clone-D2S9R (1:1000) Rabbit anti-CD19 (Cell Signaling Technology ,90176) Clone-D4V4B (1:1500) Rabbit anti-CD8 (Cell Signaling Technology, 98941) Clone-D4W2Z (1:1000) Mouse anti-Troponin T (ThermoFisher Scientific, MS-295) Clone- 13-11 (1:250) Rat anti-CD3 (Bio-Rad Laboratories, MCA1477T) Clone-CD3-12 (1:600) Rabbit anti-Myeloperoxidase (DAKO, A0398) Polyclonal (1:1500)
Validation	All antibodies are commercially available and validated by the manufactures for the applications and species used in this study. See manufactures websites for validation statements (www.abcam.com; www.cellsignal.com; www.thermofisher.com/antibody/primary; www.bio-rad-antibodies.com; www.agilent.com/en/product/immunohistochemistry/antibodies-controls)

Eukaryotic cell lines

Policy information about cell lines

Cell line source(s)	Phoenix-ECO cells were purchased directly from ATCC (ATCC CRL-3214)
Authentication	Cell lines are authenticated by ATCC (ATCC CRL-3214)
Mycoplasma contamination	We routinely test for mycoplasma contamination, the most recent results showing no contamination in any cell lines used
Commonly misidentified lines (See ICLAC register)	No commonly misidentified cell line was used

Animals and other organisms

Policy information about studies involving animals; ARRIVE guidelines recommended for reporting animal research

Laboratory animals	All mice used were on a C57Bl/6 background. C57Bl/6 were obtained from Charles River Laboratories (Wilmington, MA) PeriostinMCM mice were obtained from the laboratory of Jeffery Molkentin (Cincinnati Children's) RosaOVA mice were obtained from the laboratory of Gregory Sonnenberg (Weill Cornell Medicine) Mdx/mTRKO mice were obtained from the laboratory of Foteini Mourkioti (University of Pennsylvania) OT-I mice were obtained from The Jackson Laboratory (Bar Harbor, ME)
Wild animals	This study did not involve wild animals.
Field-collected samples	This study did not involve field-collected samples.

Human research participants

Policy information about studies involving human research participants

Population characteristics

	Donors	Explants
N	122	116
Age (years)	58±13	53±9
Female Gender	66(54)	40(34)
Patient Height (cm)	167±15	170±15
Patient Weight (kg)	84±22	77±18
Heart Weight (g)	417±115	510±134
Left ventricular Ejection Fraction (%)	58±11	20±12

Recruitment	Patients were recruited based on availability. We are unaware of any self-selection bias.